Available online at www.sciencedirect.com
ScienceDirect
Antiviral Research 73 (2007) 50–59
Antiviral Research
www.elsevier.com/locate/antiviral

A cell-based luminescence assay is effective for high-throughput screening of potential influenza antivirals

James W. Noah *, William Severson, Diana L. Noah, Lynn Rasmussen, E. Lucile White, Colleen B. Jonsson

Southern Research Institute, Drug Discovery Division, 2000 Ninth Avenue South, Birmingham, AL 35205, United States

Received 24 May 2006; accepted 12 July 2006

Abstract

The spread of highly pathogenic avian influenza across geographical and species barriers underscores the increasing need for novel antivirals to compliment vaccination and existing antiviral therapies. Identification of new antiviral lead compounds depends on robust primary assays for high-throughput screening (HTS) of large compound libraries. We have developed a cell-based screen for potential influenza antivirals that measures the cytopathic effect (CPE) induced by influenza virus (A/Udorn/72, H3N2) infection in Madin Darby canine kidney (MDCK) cells using the luminescent-based CellTiter Glo system. This 72 h assay is validated for HTS in 384-well plates and performs more consistently and reliably than methods using neutral red, with Z values > 0.8, signal-to-background > 30 and signal-to-noise > 10. In a blinded pilot screen (n = 10,781) at 10 μM concentration, four compounds (with previously demonstrated efficacy against influenza) inhibited viral-induced CPE by >50%, with EC_{50}/CC_{50} values comparable to those determined by other cell-based assays, thereby validating this assay accuracy and ability to simultaneously evaluate compound cellular availability and/or toxicity. This assay is translatable for screening against other influenza strains, such as avian flu, and may facilitate identification of antivirals for other viruses that induce CPE, such as West Nile or Dengue.

Keywords: Influenza; Antiviral; HTS; High-throughput screening; Cytopathic effect; CellTiter Glo

1. Introduction

Influenza (Orthomyxoviridae) viruses cause acute respiratory distress commonly known as "flu". Influenza A and B subtype viruses infect humans, resulting in approximately 36,000 deaths in the United States annually (Ford and Grabenstein, 2006), the vast majority of which occur in individuals who are over the age of 65 and/or have underlying heart, lung, or kidney disease, or diseases that result in immuno-suppression. These annual epidemics have a large economic impact, costing more than 1 billion dollars in direct costs, and 11 billion dollars including indirect costs, per year in the United States alone (Cinti, 2005). Influenza A viruses, which also infect a wide number of avian and mammalian species, are responsible for periodic widespread epidemics and pandemics, the most devastating of which occurred in 1918 and caused an estimated 20–40 million deaths worldwide, with a substantial number of deaths in ages 20–40 (Oxford et al., 2003). Because of the emergence in 1997 of avian influenza viruses that are directly transmittable to humans, preparations are being made for an potential epidemic, with a predicted 3–7-fold increase in the hospitalization and mortality rate and at least a 20-fold increase in economic impact in the United States alone (Cinti, 2005). Should a pandemic occur, the effect would be many times more devastating in regions of the world where the health care system is not comparably advanced (Cinti, 2005).

Vaccination remains the principle means for controlling influenza, but prophylactic and therapeutic antiviral drugs for influenza are widely available. However, their overwhelming use coupled with the recombination potential of the influenza genome has resulted in virus strains with high levels of resistance to some of these (amantadine and derivatives), making them unsuitable for continued use (Bright et al., 2006). Others (oseltamivir, zanamivir) are currently effective (Mungall et al., 2003) but more frequent use of these has the potential to rapidly promote resistance in new virus strains (Kiso et al., 2004; Regoes and Bonhoeffer, 2006) (an increasingly disturbing scenario observed in the case of avian influenza (de Jong et al.,

* Corresponding author. Tel.: +1 205 581 2804; fax: +1 205 581 2627.
E-mail address: j.noah@sri.org (J.W. Noah).

0166-3542/$ – see front matter © 2006 Elsevier B.V. All rights reserved.
doi:10.1016/j.antiviral.2006.07.006

2005; Gupta and Nguyen-Van-Tam, 2006)). In silico screening has proven effective in identifying compounds with specific antiviral properties (Fornabaio et al., 2003; von Itzstein et al., 1993), and many secondary (mechanistic) assays have been proposed for influenza antiviral screening, including in vitro assays for M2 ion channel function (Giffin et al., 1995), cap recognition (Hooker et al., 2003), polymerase endonucleolytic (Tomassini et al., 1994) and transcription activities (Lee et al., 2003), and neuraminidase activity (Tai et al., 1998). However, these are limited in large-scale screening efforts because of the difficulty of assay adaptation for high-throughput screening (HTS), the narrowness of target specificity, and the lack of inherent toxicity indicators. The identification rate of novel, effective antiviral drugs for use as influenza prophylactics and therapies would be increased by the development of primary HTS assays able to test broad classes of compounds against multiple targets simultaneously.

A key experimental advantage of a cell-based primary screening antiviral assay is the ability to simultaneously screen broad classes of compounds against the functions of multiple viral targets, as well as for toxicity (Westby et al., 2005) in HTS format. The growing use of cell-based HTS assays is balanced by the technical challenges in developing robust, large-scale systems, i.e., the labor intensive production of large quantities of cells and the inherent variability of assay performance due to differences in cell passage number and handling (Digan et al., 2005). Nonetheless, cell-based reporter assays against specific targets have been frequently used as screening tools for drug discovery and compound library evaluation, in combination with high-throughput formats designed to acquire maximum data in minimal time (Digan et al., 2005). Cell-based systems are also routinely used to determine viral titer, virulence, and more recently, for generation of recombinant viruses (Noah et al., 2003). A cell-based system that involves multiple viral infection and replication cycles is ideal for identifying compounds that affect each stage of the virus life cycle provided that reliable assay endpoint procedures are established. Cell death, or the cytopathic effect (CPE) induced by viral infection, is a well-documented and frequently exploited determinant for viral propagation in lytic viruses, but one which requires a reliable method for measuring CPE (McCoy and Wang, 2005).

Here, we describe a high-throughput cell-based assay that measures the influenza virus-induced CPE in Madin Darby canine kidney (MDCK) cells using luminescence measured by CellTiter Glo® Luminescent Cell Viability Kit (Promega) (Schwarz et al., 2004). This 72 h assay is adapted to 384-well plates and exhibits high Z and Z' values (the Z value is a statistical parameter used in HTS screening to evaluate and validate performance and robustness of assays (Zhang et al., 1999)), and high signal-to-background (S/B) and signal-to-noise (S/N) ratios. It was validated by screening 10,781 compounds for efficacy against influenza infection, and previously reported influenza inhibitors were blindly identified in duplicate screens and confirmed by secondary dose–response and toxicity assays. As an in vitro primary screen, this assay can identify promising lead compounds affecting any of the crucial influenza viral targets while simultaneously determining global issues that may affect compound efficacy (e.g. compound exclusion from the cell and/or toxicity). The method is also applicable for other influenza strains, such as avian flu, and is a simple, highly effective, and timely addition to the tools for investigating influenza strain susceptibility and virulence. It may also be used in assays to explore other viruses that induce CPE, such as West Nile, Dengue, and HIV.

2. Materials and methods

2.1. Influenza virus culture

Influenza strain A/Udorn/72 was generated using a reverse genetics system (Noah et al., 2003; Takeda et al., 2002). The supernatant from transfected MDCK cells was used to infect a fresh MDCK cell field, and a single plaque was selected and resuspended in serum-free Dulbecco's modified Eagle's medium (DMEM, Invitrogen, Carlsbad, CA) containing 1% bovine serum albumin (BSA, Invitrogen 15260-037, Fraction V) (Noah et al., 2003). The plaque-purified virus was used to innoculate 10-day embryonated chicken eggs (SPF grade, Charles River Laboratories, Wilmington, MA) (Noah et al., 2003). After inoculation, infected eggs were incubated for an additional 2 days and then placed at 4 °C overnight to terminate the embryo. The following day the egg allantoic fluid was recovered (5–10 ml/egg), solid debris was removed by centrifugation, and the fluid was aliquoted and stored below −70 °C for use in assay development and validation.

2.2. Cell culture

Madin Darby canine kidney (MDCK) cells were obtained from American Type Culture Collection (Manassas, VA, CCL-34, passage 55) and cultured in Eagle minimum essential medium (MEM, Invitrogen) with 2 mM L-glutamine and Earle's BSS adjusted to contain 1.5 g/l sodium bicarbonate, 0.1 mM non-essential amino acids, and 1.0 mM sodium pyruvate, with 10% fetal bovine serum. Cells used for the assay development and validation were not used past passage 72. The cells were grown to 90% confluency, trypsinized, and recovered. The trypsin was neutralized with cell culture media (above). The cells were centrifuged, washed twice with phosphate-buffered saline (PBS), then resuspended at 3×10^5 cells/ml in assay media (DMEM, without phenol red) containing 4.5 g/l glucose, supplemented with 4 mM L-glutamine, 100 U/ml penicillin, 100 μg/ml streptomycin, 1% BSA, which was used for all subsequent assay development and validation. The acid and base forms of phenol red absorb at 440 and 560 nm, respectively (Otto et al., 2005), which can potentially interfere with neutral red absorbance quantitation (540/405 nm), and was therefore omitted during assay development. Finally, cells were plated by automation (Matrix WellMate, Hudson, NH) and incubated at 37 °/5.0% CO_2 for 24 h prior to compound and/or virus addition.

2.3. Plaque assays

Viral titer and multiplicity of infection (MOI) values were established by plaque assays (performed as per (Noah et al.,

2003)). Briefly, 60 mm dishes containing confluent MDCK cell monolayers were infected with serially diluted egg allantoic fluid virus stock culture (prepared as in Section 2.1), incubated for 1 h to allow for virus adsorption, washed, rinsed once with PBS, then overlaid with 1× DMEM containing *N*-acetyl trypsin (Sigma, St. Louis, MA, 2.5 μg/ml) and 1% agarose. The cultures were incubated at 37 °C/5% CO_2 for 72 h, after which the agarose was removed, the cells were fixed with 4% paraformaldehyde and stained with crystal violet. Plaques were counted to establish plaque-forming units/ml (PFU/ml) in the virus stock egg allantoic fluid.

2.4. Establishment of cultured influenza virus $TCID_{50}$

The $TCID_{50}$ (50% tissue culture infectious dose, the virus stock dilution that induces CPE in 50% of the cells at endpoint) was established by serially diluting the allantoic fluid stock virus by 1/2 log dilutions onto cells in 96-well microplates, using a modified procedure adapted from (McCown and Pekosz, 2005). Cells were plated as above (3×10^5 cells/ml, 50 μl of cells/well). 24 h after plating, 50 μl of *N*-acetyl trypsin (5 μg/ml, diluted in assay media) were added to each plate well. Amplified influenza virus in egg allantoic fluid was diluted 100-fold in assay media containing 2.5 μg/ml *N*-acetyl trypsin, then added to the first column of the plate and successively serially diluted across the remaining plate columns. Fresh pipette tips were used for each dilution to avoid virus carry over to subsequent columns, and the cells in the last plate column were left uninfected as controls. The plates were incubated at 37 °C/5.0% CO_2 for 72 h. Afterward, each plate was equilibrated to room temperature (~25 °C) for 20 min, followed by addition of 100 μl of CellTiter Glo (Schwarz et al., 2004) reagent (Promega, Madison, WI) to each well. Plates were gently shaken on a plate shaker for 2 min, incubated for an additional 10 min at room temperature, then immediately analyzed in an Envision plate reader (Perkin-Elmer, Wellesley, MA) with a luminescence mirror (#2100-4040) and filter (#2100-5180). Alternatively, plates were analyzed by using neutral red, as per (Smee et al., 2002), and absorbance at 540 and 405 nm was determined on the Envision reader. Three replicate plates were analyzed; individual plates were averaged, following by averaging values of the three replicates to establish the $TCID_{50}$. The $TCID_{50}$ corresponded to a 10^6-fold dilution of the allantoic fluid virus stock. To induce CPE in 99% of the plated cells, a virus dose of 100 $TCID_{50}$s was used in all subsequent experiments (corresponding to a 1:10,000 dilution of virus stock), and this dilution was adjusted linearly from the 100 μl volume in a 96-well plate well to a 30 μl volume in a 384-well plate well. The same virus stock was used throughout the assay development and validation.

2.5. Compound handling

A proprietary 10,781 compound library (Southern Research Institute, Birmingham, AL) was used for HTS assay validation. Compounds (stored in 100% dimethyl sulfoxide (DMSO)) were diluted into assay media (prepared as above) by automation and added to the plates in 5 μl volumes using a Biomek FX liquid handler (Beckman Coulter, Fullerton, CA). The final compound concentration used in primary screening was 10 μM, with a final DMSO concentration of 0.5%.

2.6. Assay conditions

Cells (3×10^5 cells/ml, 20 μl/well) were plated in 384-well plates (as above) and incubated at 37 °C/5.0% CO_2 for 24 h prior to drug addition to allow the cells to adhere to and form a monolayer on the bottom of the well. Five microliters of each test compound (diluted in assay media for a final plate well concentration of 10 μM) were added to the plates (one compound per well), for a final plate well DMSO concentration of 0.5%. Within 10 min of compound addition, 5 μl of diluted virus (100 $TCID_{50}$ doses, diluted from amplified virus stock in egg allantoic fluid into assay media containing 15 μg/ml of *N*-acetyl trypsin, for a final virus stock dilution of 1:10,000 and a final *N*-acetyl trypsin concentration of 2.5 μg/ml) were added by automation (Matrix WellMate) to the required plate wells, which corresponds to an MOI of 0.005 PFU/cell (based on initial cell plating density of 6000 cells/well). The final assay volume was 30 μl/well in a 384-well plate. Plates were incubated at 37 °C/5.0% CO_2 for 72 h then allowed to equilibrate to room temperature for 30 min. Afterward, 30 μl of CellTiter Glo reagent was added to each plate well, and the plates were incubated at room temperature for 10–30 min before being read by luminescence detection as above (Envision, Perkin-Elmer, Wellesley, MA). The stability of relative luminescence values was determined as >3 h.

2.7. Influenza inhibitors

Ribavirin (#196066, MP Biomedicals, Solon, OH) and oseltamivir carboxylate (synthesized at Southern Research Institute) were tested as influenza inhibitors. Cells (3×10^5 cells/ml, 20 μl/well) were plated in 384-well plates (as above) and incubated at 37 °C/5.0% CO_2 for 24 h prior to drug addition. The drugs were two-fold serially diluted in assay media, with final well concentrations ranging from 0.8 to 420 μM (0.1 to 100 μg/ml, ribavirin) or 0.1 to 20 μM (0.03 to 6 μg/μl, oseltamivir carboxylate). Five microliters of each drug serial dilution were added by automation (Biomek FX) to the cells in designated plate wells, with a final DMSO concentration in each well of 0.5%. Immediately following drug addition, 5 μl of virus (100 $TCID_{50}$s in assay media containing 15 μg/ml *N*-acetyl trypsin) was added to each well (by Matrix Wellmate), for a final virus stock dilution of 1:10,000 and a final *N*-acetyl trypsin concentration of 2.5 μg/ml. The EC_{50} value (the effective drug concentration which reduces viral-induced CPE by 50%) for each inhibitor was determined at 24, 48, and 72 h post-infection. Sixteen replicates were performed on each plate, and triplicate plates were assayed for each timepoint.

2.8. Secondary confirmation assays

Dose–response (with virus) and compound toxicity assays (without virus) were performed on identified hits for confirmation of compound efficacy against influenza virus-induced CPE

and for EC_{50} and CC_{50} (drug concentration that is cytotoxic to 50% of the cells) establishment. The assay was done similarly to the primary assay conditions detailed above in Section 2.6, with the following exceptions: for dose–response assays the compound drugs were added to assay media by two-fold serial dilutions, and then added to the plate wells for a final well compound concentration ranging from 60 to 0.1 μM and a final DMSO concentration ≤1%.

2.9. Data acquisition and analysis

Raw data was imported to Activity Base Data Management software (IDBS, Alameda, CA) for determination of Z, Z', S/B, S/N, and percent inhibition for assayed compounds. Compounds showing greater than 30% inhibition of viral-induced CPE were considered "hits" and tested in secondary confirmation assays (as above). Statistical calculations were made as follows: $Z = 1 - ((3\sigma_c + 3\sigma_v)/|\mu_c - \mu_v|)$, where μ_c is the mean cell control signal, σ_c the standard deviation of the cell control signal, μ_v the mean virus control signal, and σ_v is the standard deviation of the virus control signal. $Z' = 1 - ((3\sigma_d + 3\sigma_v)/|\mu_d - \mu_v|)$, where μ_d is the mean ribavirin control signal, σ_d is the standard deviation of the ribavirin control signal. Signal-to-background (S/B, fold increase) $= \mu_c/\mu_v$. Signal-to-noise (S/N) $= (\mu_c - \mu_v)/((\sigma_c)^2 + (\sigma_v)^2)^{1/2}$ (Ghosh et al., 2005; Zhang et al., 1999). Each assay validation step was performed in triplicate with the exception of the validation screens of 10,781 compounds, and dose–response and toxicity screens, which were performed in duplicate.

3. Results

3.1. Assay development

We developed and validated an in vitro cell-based assay for high-throughput screening of diverse compound libraries for efficacy against influenza virus. During assay development, we defined optimum endpoint (CPE) detection method, optimum plating density, assay DMSO tolerance, optimum MOI, equivalency to other established CPE detection methods (neutral red uptake assay) and positive control drug choice. HTS validation included establishment of the coefficient of variation (CV) and Z values, S/B, S/N, edge and liquid handling effects, and reagent and read stability, and was completed by duplicate screening of a 10,781 compound library. Each development step was performed in triplicate, and validation steps were performed in duplicate unless otherwise noted.

To measure viability of influenza-infected cells in cell culture, we employed the commercially available CellTiter-Glo Luminescent Cell Viability Kit. Determination of cell viability is based on quantitation of adenosine triphosphate (ATP) as an indicator of metabolically active cells. The procedure involves adding the single reagent (a combination of detergent and luciferase-based enzyme) directly to previously cultured cells, resulting in cell lysis and the production of a bioluminescent signal proportional to the amount of ATP present (Schwarz et al., 2004), with the caveat that compounds that inhibit both luciferase and influenza replication will inherently give a negative signal. Initially, we determined the range of detection using MDCK cells in a 384-well plate well (assayed immediately post-plating) by assaying increasing amounts of MDCK cells to 384-plate wells in a constant volume (30 μl), followed by addition of an equal volume of CellTiter Glo reagent. Fig. 1 (line graph) shows that the range of detection from 600 up to 20,000 cells/well is linear, in good agreement with previous reports (Larson et al., 2004). Based on this, we chose an plating cell density of 6000 cells/well, then subsequently determined whether uninfected MDCK cells plated at this density continue to grow in assay media (containing 2.5 μg/ml *N*-acetyl trypsin) and if so, whether the maximum luminescence signal at 96 h post-plating (which corresponds to 72 h post-infection, the expected HTS assay endpoint time) was within established linear range of detection. Fig. 1 (gray shading) also shows the assay range of luminescence signal (corresponding to increase cell viability) assayed at 0–96 h post-plating in assay media. Maximum luminescence signal was observed at 72 h post-plating (data not shown), at which time the cells were visually confirmed to be >95% confluent in the well. Only a moderate increase in signal (5–7%) was observed beyond this time. These findings indicate that although MDCK cells still grow in assay media (with a doubling time ~48 h, which is likely due to the substitution of fractionated bovine serum albumin (BSA) for fetal calf serum during the assay), the maximum cell density and resulting luminescent (viability) signal at assay endpoint falls within the experimental linear range of detection.

For large-scale screening, compound libraries are generally stored in DMSO, which at higher concentrations (>1%) has been shown to dramatically affect both membrane permeability (Irvine et al., 1999) and influenza virus budding (Hui and Nayak,

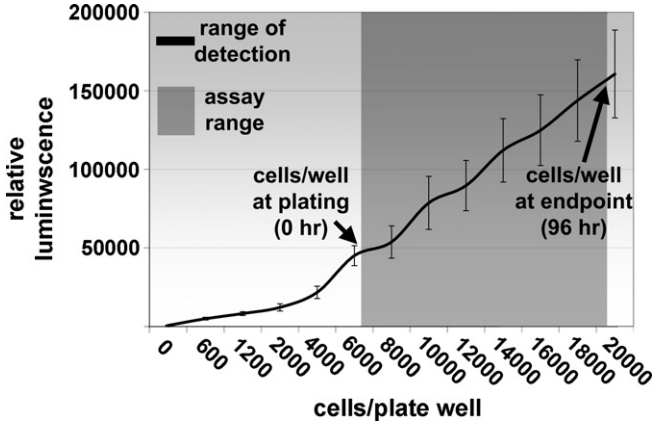

Fig. 1. Determination of endpoint reagent range of detection and assay range. Increasing amounts of MDCK cells (in a constant volume of 30 μl/well) were plated in a 384-well microtiter plate, and an equal volume of the endpoint reagent CellTiter Glo (Schwarz et al., 2004) was added to the cells immediately post-plating to determine the linear range of detection for cell viability determination. The line graph shows that the linear range of detection extends beyond 20,000 cells/well. Error bars indicate the range of values from triplicate experiments. Gray shading indicates the assay range by determining the luminescent signal (and relative cell viability) immediately post-plating (0 h, plated at 6000 cells/well), and at 96 h post-plating (72 h post-infection, assay endpoint time). Assay conditions are within the linear range of detection.

2001) in MDCK cells. To determine the effects of DMSO on cell viability and virus-induced CPE, we added DMSO to cells in increasing 0.1% increments, from 0 to 3% final DMSO concentration. After 72 h, the cells tolerated DMSO concentrations up to 2% without significant decline in total luminescence signal (data not shown). Virus-induced CPE was moderately affected, with ~4% cell viability observed below 1% DMSO versus ~8% cell viability above 1% DMSO, for virus-infected cells (data not shown). Based on these data, subsequent assay conditions were designed to keep the DMSO concentration below 0.5% during primary screening and below 1% during dose–response confirmation to prevent solvent toxicity.

It was essential for optimum assay sensitivity to establish the multiplicity of infection (MOI) required for >99% CPE in the MDCK cells at endpoint (72 h post-infection). A low MOI for multiple cycles of viral replication has been previously used for influenza-CPE assays (Smee et al., 2002) and is required to identify compounds that inhibit any stage of the virus life cycle. Typical MOI values for multiple-cycle replication assays range from 0.001 to 0.005 (Noah et al., 2003), with maximum virus production between 24 and 48 h, after which the detachment and presumed death of the remaining cells causes a slight decline in virus titer (Noah et al., 2003). We initially used serial dilutions of the allantoic fluid virus stock in plaque assays to establish the number of plaque-forming units/ml (PFU/ml), and established the viral titer in the stock (~10^7 PFU/ml, data not shown). Subsequently, we determined by two different methods (neutral red absorbance and CellTiter Glo luminescence) the amount of virus stock needed to reduce cell viability by 50% (tissue culture infectious dose 50%, or $TCID_{50}$) at 72 h post-infection in 96-well plates. Fig. 2A shows the $TCID_{50}$ plot of cell viability versus increasing concentration of added viral stock determined both by neutral red assay and CellTiter Glo assay. By both determinations the $TCID_{50}$ corresponded to a 10^6-fold dilution of virus stock allantoic fluid, indicating that, in this assay system, CellTiter Glo reagent is as accurate for MDCK cell CPE determinations as neutral red. By correlating this value with the results of the plaque assay, the $TCID_{50}$ equaled 0.3 PFU/6000 cells (based on initial cell plating density), for an MOI of 5×10^{-5} PFU/cell. To ensure CPE in 99% of the plated cells, a virus dose of 100 $TCID_{50}$s was used in all subsequent experiments (100 $TCID_{50}$s, MOI = 0.005 PFU/cell, which corresponding to a 1:10,000 dilution of virus stock), and this dose was adjusted linearly from the 100 μl volume in a 96-well plate well to a 30 μl volume in a 384-well plate well. Using this virus MOI, we determined the assay window of detection (S/B) using both neutral red and CellTiter Glo. Fig. 2B shows the progression of viral-induced CPE in MDCK cells determined at 24 h intervals, and lists the calculated S/B corresponding to each endpoint method and time point. Using CellTiter Glo, we observed the greatest increase in CPE between 24 h (cell viability = 88%) and 48 h (cell viability = 14%) post-infection. At 72 h post-infection, cell viability was determined to be 0.9%. The neutral red endpoint method determined similar 24 h (cell viability = 96%), 48 h (cell viability = 21%), and 72 h (cell viability = 1.1%) values. These findings indicate both the equivalency to and the greater ease of use of the CellTiter Glo detection method over neutral red.

3.2. Positive control drug EC_{50} values

Next, we assessed positive inhibition control drugs for assay performance by establishing the EC_{50} values for two documented influenza antivirals: ribavirin (Sidwell et al., 2005) and oseltamivir carboxylate (Tai et al., 1998). Compounds were twofold serially diluted in assay media then added to the plated cells, followed by immediate addition of influenza virus. At 24 h intervals, triplicate 384-well plates for each drug were assayed with CellTiter Glo and luminescence values were read. Fig. 3A and B show the dose–response curves versus influenza for ribavirin and oseltamivir carboxylate, respectively, at 24, 48, and 72 h post-infection, in which the % infected cell viability values were compared to those of uninfected cells and each time point was graphed against drug concentration. Twenty-four hours post-infection, EC_{50} values were indeterminate due to the lack of viral-induced CPE. Forty-eight hours post-infection, the EC_{50} values of ribavirin and oseltamivir carboxylate were 41 μM (10 μg/ml) and 1 μM (0.3 μg/ml), respectively and 72 h post-infection, those values were 66 μM (16 μg/ml) and 4 μM

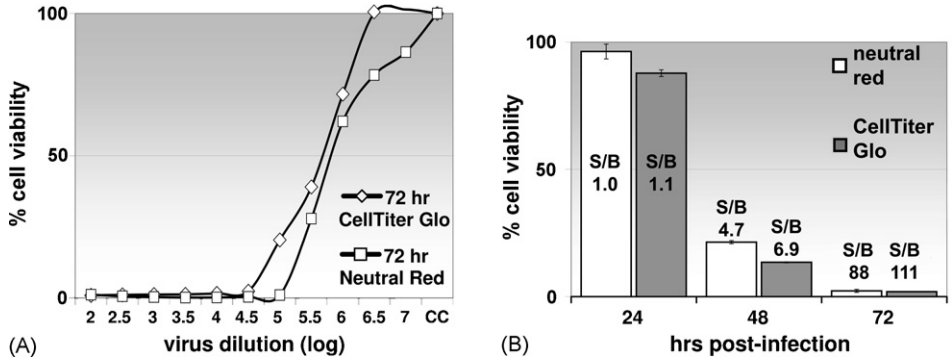

Fig. 2. Influenza strain A/Udorn/72 $TCID_{50}$ and detection window vs. time. Panel A shows that a ~10^6-fold dilution (intersection of curves and the 50% cell viability point) of the cultured virus stock (influenza virus strain A/Udorn/72 in egg allantoic fluid) caused CPE in 50% of cells when determined 72 h post-infection by both neutral red uptake (squares) and CellTiter Glo (diamonds). The corresponding virus titer of the stock was 10^7 PFU/ml, determined by plaque assays of the cultured virus stock. In panel A, CC indicates the uninfected cell control. Panel B shows % cell viability vs. time for influenza-infected MDCK cells in assay media, as determined by neutral red uptake (white bars) and CellTiter Glo (gray bars). One hundred $TCID_{50}$'s were added to each plate well, which corresponds to an MOI of 0.005 PFU/cell. S/B values determined by each assay method are indicated for each timepoint. In panel B, error bars indicate the range from triplicate experiments.

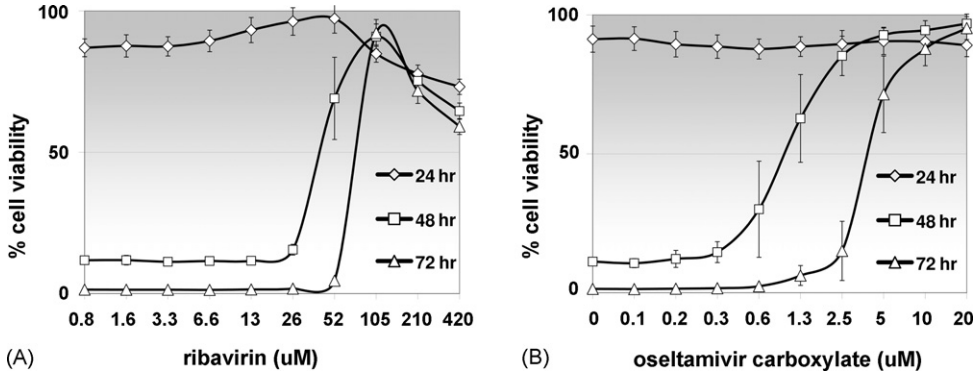

Fig. 3. Dose–response of positive control drugs. Two drugs effective against H3N2 influenza strains (Sidwell et al., 2005; Tai et al., 1998) were evaluated in dose–response experiments for EC_{50} stability, and cell toxicity. Increasing concentrations of ribavirin (0.8–420 μM; 0.2–100 μg/ml) (A) and oseltamivir carboxylate (0.05–20 μM; 0.03–6 μg/ml) (B) were added to MDCK cells, followed by virus addition (100 $TCID_{50}$s). CellTiter Glo reagent was added 24 h (diamonds), 48 h (squares), and 72 h (triangles) post-infection. The EC_{50} is determined as the point at which the drug titration curve intersects with the 50% cell viability mark. In each panel, error bars indicate the range from triplicate plates.

(1.2 μg/ml). Previously reported EC_{50} values for oseltamivir carboxylate (Smee et al., 2001) and ribavirin (Sidwell et al., 2005) (assayed with neutral red and an H3N2 influenza virus strain) range from 0.01 to 0.5 μM for oseltamivir carboxylate and 2.7 to 5.5 μg/ml (11 to 23 μM) for ribavirin. Both ranges are within three-fold of values reported here, with the difference most likely due to virus strain-dependent variation in drug susceptibility. However, ribavirin also showed toxicity above ~100 μM (25 μg/ml). Again, for the significant observed increase in S/B at 48 h versus 72 h post-infection, we standardized the assay endpoint time at 72 h. Toxicity notwithstanding and combined with the advantages of commercial availability and economy, we also chose ribavirin as the positive control drug for primary screening, at a concentration of 164 μM (40 μg/ml).

3.3. HTS adaptation and validation

After assay optimization at the bench level, our next steps were adaptation to an HTS format, appraisal of the robustness, and final validation by screening a 10,781 compound library. Initial strategies focused on developing and validating automated liquid handling methods for the reproduction of the bench level methods. This was followed by monitoring the intra- and inter-run variability of the assay (determined by the Z-factor (Zhang et al., 1999)) by running three Z-plates on three separate days, for a total of nine plates. In a separate experiment, we verified reagent stability (virus stability in assay media was >6 h) by running three Z-plates on the same day (estimated 6 h, batch size), measured at 1 h intervals (data not shown). Simultaneously, we evaluated the read stability of the CellTiter Glo reagent (tested as >3 h) by reading the same set of plates at hour intervals (data not shown). Additional HTS variables included monitoring plate coefficient of variations (average CV of positive cell controls <10%), S/B (>30) and S/N (>10) values, and moderating-edge effects due to evaporation (<10% variation in luminescence values in edge wells). Continued assay quality assessment included well-to-well, plate-to-plate and day-to-day reproducibility, as evaluated by the historical mean-of-signal (cells only) and mean-of-background (cells + virus) values (see Fig. 4A). The HTS influenza assay was validated by duplicate screening of a proprietary library containing 10,781 compounds in single-dose format, followed by dose–response confirmation of compounds that reduced CPE by >50% in the single-dose screen.

Table 1 shows the hit rate and dose–response confirmation rate for duplicate screens of the 10,781 compound library. Z, Z', S/B, S/N, hit rates for compounds that inhibited CPE above 30% and 50%, and the correlation of hits from duplicate screens are listed. A Pearson product moment correlation run on the duplicate screens gave a correlation coefficient of 0.699 with a P value <0.005. The noise level for the screen, defined as three times the standard deviation of the % inhibition of all the compounds, was 9.0%. Fig. 4A graphically illustrates the reproducibility and signal window robustness derived from the averaged control well values from each plate, and B shows the hit correlation of duplicate screens, plotted using compounds in either screen that inhibited CPE by more than 30%. Overall, we observed an average 0.14–0.19% hit rate for compounds that

Table 1
Summary of the influenza antiviral HTS assay validation

	Screen 1	Screen 2
n	10781	10781
Z[a,b]	0.80 ± 0.06	0.66 ± 0.07
Z'[a,b]	0.61 ± 0.02	0.69 ± 0.01
S/B[a,b]	36 ± 6.5	42 ± 9.4
S/N[a,b]	19 ± 5.3	9.9 ± 1.9
Primary screen ≥30% hit rate[a,c]	0.14% (n = 15)	0.19% (n = 20)
≥30% hit rate correlation coefficient[d]	0.60	P = <0.005
Primary screen ≥50% hit rate[a,c]	0.07% (n = 8)	0.07% (n = 8)
≥50% hit rate correlation coefficient[d]	0.88	P = <0.005

Dose–response confirmation of ≥50% hit rate 88%.

[a] Values for Z, Z', S/B, S/N, and primary screen hit rates are averaged from duplicate screens of thirty-eight 384-well plates each. Standard deviations are given as ± values.

[b] Calculations for Z, Z', S/B, and S/N are detailed in Section 2.9.

[c] Hit rate is based on the number of compounds that reduced viral-induced CPE by ≥30% or ≥50%, respectively, in a single screen.

[d] Correlation of compounds that reduced CPE by ≥30% or ≥50%, respectively, in both screens.

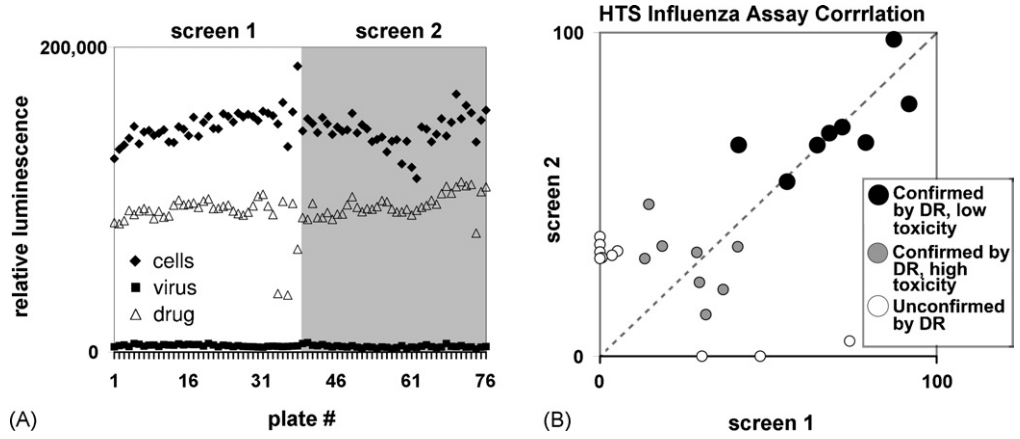

Fig. 4. Validation of primary screening and hit correlation. A library of 10,781 compounds was screened in duplicate to validate performance of the influenza HTS assay. Panel A shows the averaged values (relative luminescence) for control wells in the 76 plates of the duplicate validation screens (plates 1–38 of the first replicate screen are unshaded, and 39–76 of the second replicate screen are shaded). Points on the graph are indicated as wells containing MDCK cells only (diamonds cells), wells containing cells infected with influenza virus (squares virus), and wells containing cells infected with influenza virus in the presence of 40 μg/ml ribavirin (triangles drug). Statistical information for the duplicate screens can be found in Table 1. Panel B shows the abbreviated hit results for compound screening. The scatter plot shows the % CPE inhibition of screened compounds observed in screen 1 plotted against that observed for the same compounds in screen 2. Compounds that inhibited CPE by >30% in either replicate screen are shown as dots on the scatter plot. Hollow dots indicate compounds that were not confirmed by subsequent dose–response (DR) experiments. Gray dots indicate compounds that were confirmed by dose–response but also exhibited cellular toxicity at higher concentrations. Large black dots indicate compounds that were confirmed in dose–response with minimal cellular toxicity. Correlation coefficients and statistical significance (*P* value) for the entire compound set are indicated in Table 1.

inhibited CPE by >30%, with 62% correlation of hits between replicates. The hit rate for compounds that inhibited CPE by >50% (Fig. 4B, black dots) was 0.08%, with an 88% confirmation of hits by dose–response. Of the six unique compounds in this category, one was oseltamivir carboxylate (as a double-blinded control), one was unconfirmed by dose–response, one was carbocyclic cytidine, two were 6-azauridine derivatives, and one was a substituted pyrazine compound (T-705). These latter four compounds have all previously been reported as effective inhibitors of influenza replication (Furuta et al., 2005; Shannon et al., 1981; Smee et al., 2002), and their dose–response confirmation further validates the influenza assay sensitivity and performance. Fig. 5 shows the EC_{50}, CC_{50} and calculated SI values for these four antivirals. The previously reported EC_{50} values for carbocyclic cytidine (2.5 μg/ml, or 11 μM), 6-azauridine (3.1 μM) and T-705 (1.0 μM) by neutral red absorbance assay are in close agreement with the values reported using this assay system, with exception of that of carbocyclic cytodine, which

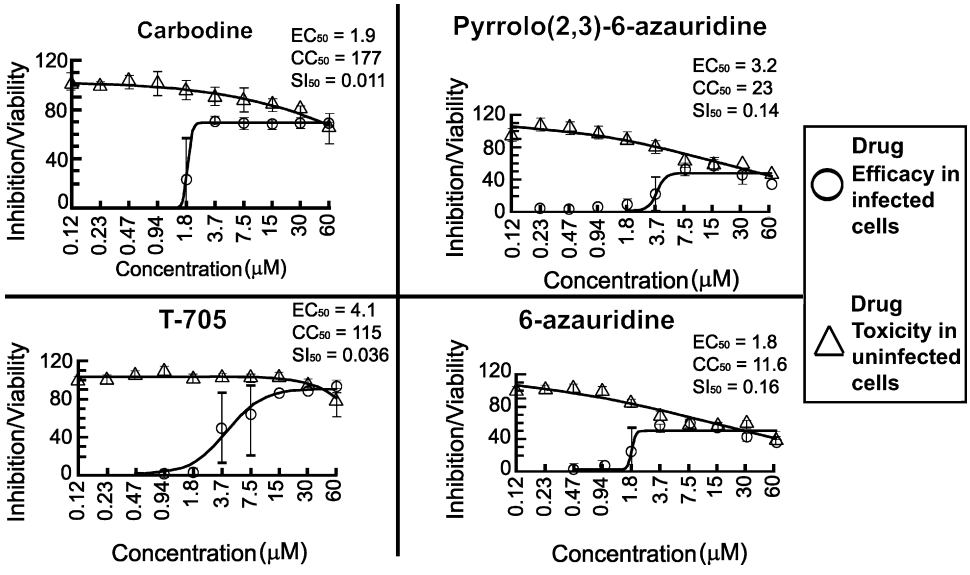

Fig. 5. Dose–response confirmation of identified influenza inhibitors. A blind screen of 10,781 compounds identified several that inhibited influenza-induced CPE. Four of these were confirmed by dose–response (circles), and were recognized as previously characterized inhibitors of influenza replication in cell culture. The EC_{50} values are shown for carbocyclic cytodine (Shannon et al., 1981) pyrrolo-(2,3)-6-azauridine, 6-azauridine (Smee et al., 2002), and T-705 (Furuta et al., 2005). In parallel experiments, CC_{50} values (triangles) and selective indices ($SI = CC_{50}/EC_{50}$) were also determined, and are indicated for each compound. In each panel, error bars indicate the range from triplicate experiments.

was previously assayed by visual scoring of CPE (Shannon et al., 1981). Close examination of the curves shows that only T-705 (Fig. 5) achieves an EC_{90} value (the effective drug concentration which prevents viral-induced CPE in 90% of the cells) ranging from 7 to 35 μM in duplicate screens, while the other three compounds never reach the 90% effective range, most likely due to the observed cellular toxicity of these compounds at higher concentrations. These results indicate that the HTS assay is competent at accurately identifying both the efficacy and potential toxicity of compounds.

4. Discussion

This CPE-based HTS assay design was evaluated on three logistical criteria: (1) robustness with a high degree of reproducibility and low deviation; (2) high sensitivity, low background, and capable of evaluating a broad range of compounds; (3) adaptability for screening large compound libraries. The greatest contribution to sensitivity and low background is the CellTiter Glo endpoint reagent as a measure of cell viability. This CPE determination method has a great advantage over the neutral red uptake assay in that the single reagent addition protocol is easily adaptable to HTS. The choices of cell type and virus strain were also critical considerations for assay robustness accuracy, and reproducibility. Madin Darby canine kidney (MDCK) cells have been routinely used to culture influenza for virulence testing, and their reaction to influenza infection, including their rapid and near complete cell death as a result, has been well characterized not only in context as a viable host of influenza infection (Noah et al., 2003), but also as a common model for studying cell growth regulation, metabolism (Horster and Stopp, 1986), and membrane permeability (Irvine et al., 1999). In a 384-well format, MDCK cells have a reduced growth rate in assay media (doubling time ∼48 h), which may contribute to assay stability by decreasing artifacts induced by rapidly metabolizing cells (e.g. plating time windows and % confluency) (Fursov et al., 2005) and have been shown to be viable for extended periods of time (>72 h) in serum-containing media in up to 1% DMSO (Irvine et al., 1999). Higher DMSO concentrations (>1%) have been shown to specifically affect budding of influenza virus by modulating membrane permeability (Hui and Nayak, 2001), thereby decreasing viral-induced CPE. We observed a high tolerance to DMSO in assay media, and the cells survived in up to 2% DMSO for >72 h with only a two-fold decrease in viral-induced CPE at the same DMSO concentration. This high MDCK cell DMSO tolerance provides an advantage during dose–response confirmation by allowing higher screening concentrations of compounds (and corresponding DMSO solvent).

An appropriate influenza viral strain was another crucial assay component. To promote assay robustness and reproducibility, strain A/Udorn/72 (H3N2) was chosen. Like MDCK cells, this strain is also well characterized and has been extensively used as a model for studying the functions of individual viral components in cell culture (Takeda et al., 2002), and the efficacy of vaccines in animals models (Ozaki et al., 2005). Because H3N2 strains have previously shown a higher drug sensitivity compared to H1N1 strains (Sidwell and Smee, 2000; Smee et al., 2001), their use may increase the chance of identifying inhibitors which may be less effective (and therefore unrecognized) by other influenza strains. Also, the use of a laboratory-adapted strain minimizes safety concerns when dealing with the possibility of an HTS instrument malfunction, which may result in equipment contamination and require decontamination. This combination of cell type and virus strain resulted in a high degree of reproducibility and low deviation, while still maintaining sensitivity (determined by sensitivity to both control drugs and identified inhibitors).

Two antivirals, oseltamivir carboxylate and ribavirin, were evaluated based on availability and assay performance, and ribavirin was chosen as the assay positive inhibition control. Oseltamivir carboxylate blocks the active site of the viral neuraminidase surface enzyme, thereby inhibiting both the cleavage of sialic acid residues from oligosaccharide chains of cell surface receptors and the cleavage of these same residues from viral proteins, which promotes virus aggregation and prevents the release of virus progeny from infected cells (Tai et al., 1998). Ribavirin is a broad-spectrum antiviral compound reported to be active in vivo against respiratory syncytial virus (RSV), human immuno-deficiency virus (HIV), hepatitis C virus (HCV), and other infectious agents, as well as during in vitro influenza infections (Sidwell et al., 2005), and is approved for human use as an influenza antiviral therapy in Europe (Leophonte, 2005) and as an HCV antiviral combination therapy in the United States (Bartlett, 2005). Its metabolite, ribavirin 5′-phosphate, inhibits inosine monophosphate dehydrogenase (Markland et al., 2000), which may account for cytotoxicity at higher concentrations. It has also been shown to act as a potent RNA virus mutagen in poliovirus-infected cells (Crotty et al., 2000) and causes error catastrophe in hantavirus (Severson et al., 2003), and has specifically been shown to inhibit influenza virus RNA polymerase (Eriksson et al., 1977), possibly through a similar mechanism. Although oseltamivir carboxylate inhibited viral-induced CPE (>95%) and showed no toxicity at high concentrations, ribavirin is also effective at non-toxic concentrations (80% CPE inhibition at 164 μM (40 μg/ml)), inexpensive and commercially available, the latter which are significant factors in large-scale screening endeavors.

Several points can be drawn from the validation screening of the 10,781 compound library. Statistical values for assay performance (Table 1) indicate that the assay is sufficiently robust and reproducible for an HTS platform. Typically, a S/B value greater than 5 is an adequate detection window, and the Z and Z'-factors between 0.5 and 1.0 are considered robust enough for an HTS assay (Zhang et al., 1999). This assay functions well as a primary screen and also as a secondary method for investigating the toxicity, biological availability, or metabolic interference of compounds identified through influenza biochemical target-oriented assays. It is extremely stringent in its identification of influenza inhibitors, as shown from the hit rate (0.08%) of compounds that inhibited CPE by >50% (Table 1), but also extremely accurate, evidenced by the corresponding hit correlation, dose–response confirmation rates (100%), and evaluation of known antivirals. Several assay modifications can be suggested (depending on

the types of compounds screened) that may increase the hit rate, including dosing at a higher compound concentration (i.e. >10 μM) and/or reducing the assay length from 72 to 48 h. The former modification runs the risk of complications due to compound toxicity while the latter significantly decreases the assay window of detection (by >5-fold, see Fig. 2B). An alteration in the time of compound addition (pre- or post-virus addition) may also be valuable to determine whether compounds are effective against viral replication or prevention of viral entry into cells. Finally, this assay is a timely addition to the arsenal of tools available for screening against human influenza and avian influenza strains in bio-containment. Using it, we have screened >500,000 compounds against human influenza and are continuing at a rate ~90,000 compounds/week. The assay can be readily adapted for screening similar numbers of compounds against other influenza viruses, which requires re-establishment of the $TCID_{50}$ for the corresponding MOI determination, optimal time of endpoint determination, and measurement of control drug susceptibility. For H5N1 viruses, an additional assay modification includes the omission of *N*-acetyl trypsin from the assay media, due to the ability of exogenous proteases to cleave the hemagglutinin polypeptide. These methods are also directly adaptable for assays that test vaccine efficacy (microneutralization), or against other CPE-inducing viruses.

Here, a high-throughput, cell-based assay was developed, validated and employed to screen for compounds effective against influenza A virus in cell culture, using cell viability as the endpoint as determined by CellTiter Glo. The influenza strain A/Udorn/72 (H3N2) was used to induce CPE in MDCK cells (Noah et al., 2003), and ribavirin and oseltamivir carboxylate were evaluated as positive control inhibition drugs based on assay performance, cost, and commercial availability. EC_{50} values for both drugs were similar to those established by different assay methods in previous reports (Sidwell et al., 2005; Tai et al., 1998). The HTS adapted assay performed consistently and accurately, with a high secondary confirmation rate of primary screen hits. Four known inhibitors of influenza were blindly identified and verified by dose–response/toxicity secondary screening, and HTS assay established EC_{50} values were similar to those previously reported using other assay systems (Furuta et al., 2005; Shannon et al., 1981; Smee et al., 2002), therefore validating this assay. This in vitro primary HTS assay, combined with additional secondary dose–response and follow-up biochemical target assays, forms a comprehensive screening program for identifying virus strain and virus target susceptibility to novel, potential influenza and avian influenza antivirals.

Acknowledgements

This work was supported by NIH N01-AI-30047 to CBJ and NIH R01-AI-071393 and a Southeast Regional Center of Excellence for Biodefense and Emerging Infections (SERCEB) Career Development Award to JWN.

References

Bartlett, J.G., 2005. FDA approves Pegasys and Copegus for hepatitis C in patients with HIV co-infection. Hopkins HIV Rep. 17, 15.

Bright, R.A., Shay, D.K., Shu, B., Cox, N.J., Klimov, A.I., 2006. Adamantane resistance among influenza A viruses isolated early during the 2005–2006 influenza season in the United States. J. Am. Med. Assoc. 295, 891–894.

Cinti, S., 2005. Pandemic influenza: are we ready? Disaster Manage. Response 3, 61–67.

Crotty, S., Maag, D., Arnold, J.J., Zhong, W., Lau, J.Y., Hong, Z., Andino, R., Cameron, C.E., 2000. The broad-spectrum antiviral ribonucleoside ribavirin is an RNA virus mutagen. Nat. Med. 6, 1375–1379.

de Jong, M.D., Tran, T.T., Truong, H.K., Vo, M.H., Smith, G.J., Nguyen, V.C., Bach, V.C., Phan, T.Q., Do, Q.H., Guan, Y., Peiris, J.S., Tran, T.H., Farrar, J., 2005. Oseltamivir resistance during treatment of influenza A (H5N1) infection. N. Engl. J. Med. 353, 2667–2672.

Digan, M.E., Pou, C., Niu, H., Zhang, J.H., 2005. Evaluation of division-arrested cells for cell-based high-throughput screening and profiling. J. Biomol. Screen 10, 615–623.

Eriksson, B., Helgstrand, E., Johansson, N.G., Larsson, A., Misiorny, A., Noren, J.O., Philipson, L., Stenberg, K., Stening, G., Stridh, S., Oberg, B., 1977. Inhibition of influenza virus ribonucleic acid polymerase by ribavirin triphosphate. Antimicrob. Agents Chemother. 11, 946–951.

Ford, S.M., Grabenstein, J.D., 2006. Pandemics, avian influenza A (H5N1), and a strategy for pharmacists. Pharmacotherapy 26, 312–322.

Fornabaio, M., Cozzini, P., Mozzarelli, A., Abraham, D.J., Kellogg, G.E., 2003. Simple, intuitive calculations of free energy of binding for protein–ligand complexes. 2. Computational titration and pH effects in molecular models of neuraminidase-inhibitor complexes. J. Med. Chem. 46, 4487–4500.

Fursov, N., Cong, M., Federici, M., Platchek, M., Haytko, P., Tacke, R., Livelli, T., Zhong, Z., 2005. Improving consistency of cell-based assays by using division-arrested cells. Assay Drug Dev. Technol. 3, 7–15.

Furuta, Y., Takahashi, K., Kuno-Maekawa, M., Sangawa, H., Uehara, S., Kozaki, K., Nomura, N., Egawa, H., Shiraki, K., 2005. Mechanism of action of T-705 against influenza virus. Antimicrob. Agents Chemother. 49, 981–986.

Ghosh, R.N., DeBiasio, R., Hudson, C.C., Ramer, E.R., Cowan, C.L., Oakley, R.H., 2005. Quantitative cell-based high-content screening for vasopressin receptor agonists using transfluor technology. J. Biomol. Screen 10, 476–484.

Giffin, K., Rader, R.K., Marino, M.H., Forgey, R.W., 1995. Novel assay for the influenza virus M2 channel activity. FEBS Lett. 357, 269–274.

Gupta, R.K., Nguyen-Van-Tam, J.S., 2006. Oseltamivir resistance in influenza A (H5N1) infection. N. Engl. J. Med. 354, 1423–1424 (author reply 1423–1424).

Hooker, L., Sully, R., Handa, B., Ono, N., Koyano, H., Klumpp, K., 2003. Quantitative analysis of influenza virus RNP interaction with RNA cap structures and comparison to human cap binding protein eIF4E. Biochemistry 42, 6234–6240.

Horster, M.F., Stopp, M., 1986. Transport and metabolic functions in cultured renal tubule cells. Kidney Int. 29, 46–53.

Hui, E.K., Nayak, D.P., 2001. Role of ATP in influenza virus budding. Virology 290, 329–341.

Irvine, J.D., Takahashi, L., Lockhart, K., Cheong, J., Tolan, J.W., Selick, H.E., Grove, J.R., 1999. MDCK (Madin-Darby canine kidney) cells: a tool for membrane permeability screening. J. Pharm. Sci. 88, 28–33.

Kiso, M., Mitamura, K., Sakai-Tagawa, Y., Shiraishi, K., Kawakami, C., Kimura, K., Hayden, F.G., Sugaya, N., Kawaoka, Y., 2004. Resistant influenza A viruses in children treated with oseltamivir: descriptive study. Lancet 364, 759–765.

Larson, B., Worzella, T., Gallagher, A., Matthews, E., 2004. Miniaturizing and automating cell viability and reporter assays for high-throughput and ultrahigh-throughput screening. Cell Notes (Promega), 10–14.

Lee, M.T., Klumpp, K., Digard, P., Tiley, L., 2003. Activation of influenza virus RNA polymerase by the 5′ and 3′ terminal duplex of genomic RNA. Nucleic Acids Res. 31, 1624–1632.

Leophonte, P., 2005. Antivirals for influenza. Bull. Acad. Natl. Med. 189, 341–355 (discussion 355–347).

Markland, W., McQuaid, T.J., Jain, J., Kwong, A.D., 2000. Broad-spectrum antiviral activity of the IMP dehydrogenase inhibitor VX-497: a comparison with ribavirin and demonstration of antiviral additivity with alpha interferon. Antimicrob. Agents Chemother. 44, 859–866.

McCown, M.F., Pekosz, A., 2005. The influenza A virus M2 cytoplasmic tail is required for infectious virus production and efficient genome packaging. J. Virol. 79, 3595–3605.

McCoy, M.H., Wang, E., 2005. Use of electric cell–substrate impedance sensing as a tool for quantifying cytopathic effect in influenza A virus infected MDCK cells in real-time. J. Virol. Meth. 130, 157–161.

Mungall, B.A., Xu, X., Klimov, A., 2003. Assaying susceptibility of avian and other influenza A viruses to zanamivir: comparison of fluorescent and chemiluminescent neuraminidase assays. Avian Dis. 47, 1141–1144.

Noah, D.L., Twu, K.Y., Krug, R.M., 2003. Cellular antiviral responses against influenza A virus are countered at the posttranscriptional level by the viral NS1A protein via its binding to a cellular protein required for the 3′ end processing of cellular pre-mRNAS. Virology 307, 386–395.

Otto, W.H., Larive, C.K., Mason, S.C., Robinson, J.B., Heppert, J.A., Ellis, J.D., 2005. Using visible spectrophotometers and pH measurements to study speciation in a guided-inquiry laboratory. J. Chem. Ed. 82, 1552–1554.

Oxford, J.S., Bossuyt, S., Balasingam, S., Mann, A., Novelli, P., Lambkin, R., 2003. Treatment of epidemic and pandemic influenza with neuraminidase and M2 proton channel inhibitors. Clin. Microbiol. Infect. 9, 1–14.

Ozaki, T., Yauchi, M., Xin, K.Q., Hirahara, F., Okuda, K., 2005. Cross-reactive protection against influenza A virus by a topically applied DNA vaccine encoding M gene with adjuvant. Viral Immunol. 18, 373–380.

Regoes, R.R., Bonhoeffer, S., 2006. Emergence of drug-resistant influenza virus: population dynamical considerations. Science 312, 389–391.

Schwarz, F., Rothamel, D., Herten, M., Sculean, A., Scherbaum, W., Becker, J., 2004. Effect of enamel matrix protein derivative on the attachment, proliferation, and viability of human SaOs(2) osteoblasts on titanium implants. Clin. Oral. Investig. 8, 165–171.

Severson, W.E., Schmaljohn, C.S., Javadian, A., Jonsson, C.B., 2003. Ribavirin causes error catastrophe during Hantaan virus replication. J. Virol. 77, 481–488.

Shannon, W.M., Arnett, G., Westbrook, L., Shealy, Y.F., O'Dell, C.A., Brockman, R.W., 1981. Evaluation of carbodine, the carbocyclic analog of cytidine, and related carbocyclic analogs of pyrimidine nucleosides for antiviral activity against human influenza type A viruses. Antimicrob. Agents Chemother. 20, 769–776.

Sidwell, R.W., Bailey, K.W., Wong, M.H., Barnard, D.L., Smee, D.F., 2005. In vitro and in vivo influenza virus-inhibitory effects of viramidine. Antiviral Res. 68, 10–17.

Sidwell, R.W., Smee, D.F., 2000. In vitro and in vivo assay systems for study of influenza virus inhibitors. Antiviral Res. 48, 1–16.

Smee, D.F., Morrison, A.C., Barnard, D.L., Sidwell, R.W., 2002. Comparison of colorimetric, fluorometric, and visual methods for determining anti-influenza (H1N1 and H3N2) virus activities and toxicities of compounds. J. Virol. Meth. 106, 71–79.

Smee, D.F., Sidwell, R.W., Morrison, A.C., Bailey, K.W., Baum, E.Z., Ly, L., Wagaman, P.C., 2001. Characterization of an influenza A (H3N2) virus resistant to the cyclopentane neuraminidase inhibitor RWJ-270201. Antiviral Res. 52, 251–259.

Tai, C.Y., Escarpe, P.A., Sidwell, R.W., Williams, M.A., Lew, W., Wu, H., Kim, C.U., Mendel, D.B., 1998. Characterization of human influenza virus variants selected in vitro in the presence of the neuraminidase inhibitor GS 4071. Antimicrob. Agents Chemother. 42, 3234–3241.

Takeda, M., Pekosz, A., Shuck, K., Pinto, L.H., Lamb, R.A., 2002. Influenza a virus M2 ion channel activity is essential for efficient replication in tissue culture. J. Virol. 76, 1391–1399.

Tomassini, J., Selnick, H., Davies, M.E., Armstrong, M.E., Baldwin, J., Bourgeois, M., Hastings, J., Hazuda, D., Lewis, J., McClements, W., et al., 1994. Inhibition of cap (m7GpppXm)-dependent endonuclease of influenza virus by 4-substituted 2,4-dioxobutanoic acid compounds. Antimicrob. Agents Chemother. 38, 2827–2837.

von Itzstein, M., Wu, W.Y., Kok, G.B., Pegg, M.S., Dyason, J.C., Jin, B., Van Phan, T., Smythe, M.L., White, H.F., Oliver, S.W., et al., 1993. Rational design of potent sialidase-based inhibitors of influenza virus replication. Nature 363, 418–423.

Westby, M., Nakayama, G.R., Butler, S.L., Blair, W.S., 2005. Cell-based and biochemical screening approaches for the discovery of novel HIV-1 inhibitors. Antiviral Res. 67, 121–140.

Zhang, J.H., Chung, T.D., Oldenburg, K.R., 1999. A simple statistical parameter for use in evaluation and validation of high throughput screening assays. J. Biomol. Screen 4, 67–73.